

## ARTICLE TYPE

# A computational model for irradiance on close-in planetary systems

Mradumay Sadh<sup>1</sup> and Lorenzo Gavassino<sup>2</sup><sup>1</sup>School of Mathematical and Physical Sciences, Macquarie University, Macquarie Park, Sydney, 2109, New South Wales, Australia<sup>2</sup>Department of Mathematics, Vanderbilt University, Nashville, TN, USA

Author for correspondence: Mradumay Sadh, Email: mradumay.sadh@students.mq.edu.au.

**Abstract**

There is something about inverse-square laws that makes them fail at extremities. The inverse-square law, which is used commonly in studying the irradiance on exoplanets fails at the extreme case of planets closer than 0.01 AU. Therefore, in order to correctly predict possible climate states of such systems, we need a new model which accurately calculates angles subtended by various surface elements and integrate the generalized equation. A direct consequence of such a model is the shift of the terminator about 20 degrees beyond the poles. The irradiance at the poles is about 100–200 kW/m<sup>2</sup> higher than what is predicted by the inverse-square law. This work therefore becomes crucial because it underscores the need to modify the current GCM models. The error in the numerical integration values of irradiance is less than one percent making our estimate very reliable.

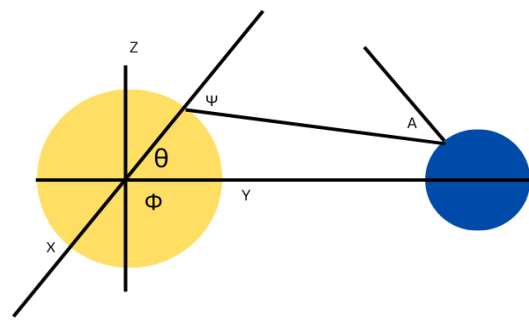
**Keywords:** Radiative Transfer, Stars:fundamental parameters, Planets and satellites:fundamental parameters

**1. Introduction**

Our goal is to estimate the irradiance of planets at an extremely close distance to their host-stars. Since 1995 we have discovered planets closer than 0.05 AU in droves. (Mayor and Queloz 1995; Léger et al. 2009; Batalha et al. 2011; Demory et al. 2011). The irradiance is an important factor in understanding the climate of an exoplanet. The extent of unreliability of the inverse-square law calls for a commensurate need for a better model. The inverse-square law is one of the founding pillars for studying radiation(Charbonneau and Noyes 2000; Guillot 2010; Kane et al. 2020). However, it turns fallacious if we incorporate the planets found very close to their host-stars. If one simply imagines such a close configuration, it is immediately clear that inverse-square law doesn't explain irradiation on the night-side of a close exoplanet since it assumes that the star is point-sized. This demands a new model that better explains the irradiation distribution and also incorporates the stellar limb darkening. In this approach, we attempt to make a robust model that accurately predicts the irradiation distribution on such planets. Our earlier conference paper (Sadh and Gavassino 2022) has the same model but the current paper has the exposition of the model aiming to consolidate our findings and results for the popular exoplanet 55 Cnc e.

The paper is structured as follows. In section 2, an equation is derived for irradiance using a 3-D geometrical formulation and limb darkening effects for a surface element on the star and then integrated for the whole star. The integration of this equation by analytic means happens to be complicated and cumbersome. Therefore, numerical integration methods are used to solve this integral. The results section depicts the effects of this model for a few close exoplanets with Sun like host-stars. Subsequently, an analysis about the cases where this model significantly differs from the IS law and the reason behind these differences is presented. Lastly, there is a discussion about the limitations of the model and its applicability.

We have derived a detailed physical explanation of how the inverse-square law is violated in the appendix. For brevity, we can summarise that the inverse-square law holds only on those regions on a planet where the flux from the star fails to be radial.

**2. Constructing a new model**

**Figure 1.** Spherical geometry of the star and planet depicting the incident ray, and normal lines to the stellar and planetary surface under consideration.

In our approach, we intend to integrate the total irradiance from each surface element on the star. Later on, we incorporate the geometric effects that affect the limits of this integration. A fairly similar approach has been taken in previous studies by (Huang and Zhou 2000), (Kopal 1954) and (Horvat et al. 2019) for calculating irradiation effects in close binary stars. However, this is the first study for the special case of a star-planet system.

### 2.1 Description of the star-planet system in 3-D geometry

Assuming the star and planet to be spherical, we choose an arbitrary point on the star and calculate the irradiance on an arbitrary point on the planet as illustrated in Fig. 1. We can express any point in Cartesian coordinates on the stellar sphere as:

$$x_s = R \cos \theta \sin \phi \quad (1)$$

$$y_s = R \cos \theta \cos \phi \quad (2)$$

$$z_s = R \sin \theta, \quad (3)$$

where  $\theta$  and  $\phi$  define the latitude and longitude of the host star, respectively. The angle  $\theta$  is measured along the YZ plane and  $\phi$  along the XY plane. Likewise, we can express any point in Cartesian coordinates on the planetary sphere as:

$$x_p = r \cos \lambda \sin \delta \quad (4)$$

$$y_p = R + r + d + r \cos \lambda \cos \delta = a + r \cos \lambda \cos \delta \quad (5)$$

$$z_p = r \sin \lambda, \quad (6)$$

where  $\lambda$  and  $\delta$  define the latitude and longitude of the planet, respectively. Here,  $d$  is the shortest distance between the surfaces of the planet and the star and  $(r + R + d)$  is the semi-major axis( $a$ ). The star is assumed to have a total bolometric luminosity  $L_b$  and effective temperature  $T_*$ . For a surface element  $dS$  on the star, the power  $dL_b$  emitted by this surface is given by the Stephan-Boltzmann law as:

$$dL_b = \sigma T_s^4 dS = \frac{L_b R^2 \cos \theta d\theta d\phi}{4\pi R^2} = \frac{L_b \cos \theta d\theta d\phi}{4\pi}. \quad (7)$$

#### 2.1.1 Deriving equation for irradiance

By definition, irradiance is the radiant flux emitted by a body per unit area on the receiving surface. The radiant flux is simply the power emitted by the source (Kingston 1995). Mathematically,

$$I = \frac{dF}{da} \quad (8)$$

Where  $F$  is radiant flux or power emitted by the star and  $da$  is the surface area on the planet. The radiant flux is related to the specific intensity as

$$F = \int_{\Omega} I_{\nu} \cos \theta d\Omega \quad (9)$$

The radiant flux is related to the radiance and étendue or throughput by the following relation

$$\partial F = l \partial G \quad (10)$$

Where  $G$  is the étendue and  $l$  is the radiance of the host star. Now, let's calculate the radiance of the star. It should be noted that the star is assumed to be a Lambertian emitter. Since the star is considered to be a black-body, we have the spectral radiance given by

$$l_{\nu} = \frac{2h\nu^3}{c^2} \frac{1}{e^{\frac{h\nu}{kT}} - 1} \quad (11)$$

Substituting this in equation 10

$$\partial F = l_{\nu} \partial G \quad (12)$$

The throughput of an optical system is given by

$$\partial G = d\sigma d\Omega \quad (13)$$

Where  $d\sigma$  is the area perpendicular to the normal vector of the emitting surface and  $d\Omega$  is the solid angle subtended by the receiving surface at the source. Coming back to the surface element on the star which is emitting radiation at an angle of  $\psi$  from its normal vector towards the planet as shown in figure 1. The receiving surface is receiving this radiation at an angle  $A$  from its normal vector. Since throughput requires the area perpendicular to the direction of propagation, we take a component of the surface element  $dS$ . Therefore,

$$\partial G = dS \cos \psi d\Omega \quad (14)$$

The solid angle subtended by the receiving surface perpendicular to the incoming radiation will be

$$d\Omega = \frac{d \cos A}{d_s^2} \quad (15)$$

Therefore,

$$\partial G = dS \cos \psi \frac{d \cos A}{d_s^2} \quad (16)$$

Substituting this back in equation 12, we get

$$\partial F = l_{\nu} dS \cos \psi \frac{d \cos A}{d_s^2} \quad (17)$$

Since the irradiance is defined as

$$I = \frac{dF}{da} \quad (18)$$

We get the general equation for irradiance through a surface element  $dS$  on the star

$$I = l_{\nu} \frac{\cos \psi \cos A}{d_s^2} dS \quad (19)$$

Where  $dS$  is given by  $R^2 \cos \theta d\theta d\phi$  as mentioned in equation 7. If we integrate this over the complete surface of the star, we get the total irradiance coming from the star

$$\int dI = \int_{\nu} \int_S l_{\nu} \frac{\cos \psi \cos A}{d_s^2} dS \quad (20)$$

If we integrate this over all frequencies, we get

$$l = \int_0^{\infty} \frac{2h\nu^3}{c^2} \frac{1}{e^{\frac{h\nu}{kT}} - 1} \quad (21)$$

Therefore,

$$l = \frac{2\pi^4 k^4 T^4}{15h^3 c^2} \quad (22)$$

Since we know the Stephan-Boltzmann constant is

$$\sigma = \frac{2\pi^5 k^4 T^4}{15h^3 c^2} \quad (23)$$

Therefore, we have

$$l = \frac{\sigma T^4}{\pi} \quad (24)$$

To make the calculations easy, we can calculate these irradiance values along the sub-stellar longitude on the planet since the planet can be considered a 2-D body in this case. Now, we evaluate the general expressions for distance ( $d_s$ ), angle A, and  $\psi$ .

## 2.2 Calculation of the distance between the stellar and planetary surfaces

For this calculation we need to evaluate the Euclidean distance between any set of arbitrary points on the star and the planet or, in other words, the length of the line segment MN in Fig.1. Using the Cartesian coordinates introduced before we have:

$$d_s = \left[ (R \sin \theta - r \sin \lambda)^2 + (R \cos \theta \sin \phi - r \cos \lambda \sin \delta)^2 + \right. \quad (25)$$

$$\left. (R \cos \theta \cos \phi - r - R - d - r \cos \lambda \cos \delta)^2 \right]^{1/2}. \quad (26)$$

## 2.3 Angle between area vector and incident ray from the surface element

The angle between the incident ray from the star (MN) and the area vector of the receiving surface is given by A as shown in Fig.1. If the direction cosines of MN and the area vector are  $l_1, l_2, l_3$  and  $m_1, m_2, m_3$  respectively, then the angle between them is derived by taking a dot product of two unit vectors along these lines:

$$\cos A = l_1 m_1 + l_2 m_2 + l_3 m_3. \quad (27)$$

The direction cosine of the area vector is given by:

$$m_1 = \frac{x_p}{r} = \cos \lambda \sin \delta \quad (28)$$

$$m_2 = \frac{y_p}{r} = \cos \lambda \cos \delta \quad (29)$$

$$m_3 = \frac{z_p}{r} = \sin \lambda. \quad (30)$$

Similarly, the direction cosine of the incident ray is given by:

$$l_1 = \frac{x_p - x_s}{d_s} = \frac{r \cos \lambda \sin \delta - R \cos \theta \sin \phi}{d_s} \quad (31)$$

$$l_2 = \frac{y_p - y_s}{d_s} = \frac{a + r \cos \lambda \cos \delta - R \cos \theta \cos \phi}{d_s} \quad (32)$$

$$l_3 = \frac{z_p - z_s}{d_s} = \frac{r \sin \lambda - R \sin \theta}{d_s}. \quad (33)$$

Using equation (27) and substituting the values of the direction cosines, we get:

$$\cos A = \frac{R[-\cos \theta \cos \lambda \cos(\phi - \delta) - \sin \theta \sin \lambda]}{d_s} + \frac{a \cos \lambda \cos \delta + r}{d_s}.$$

Similarly  $\psi$  can be calculated as:

$$\cos \psi = \frac{(a - r \cos \lambda) \cos \theta \cos \lambda + r \sin \theta \sin \lambda - R}{d_s}. \quad (34)$$

It is crucial to incorporate the essential geometrical factors which affect the limits of the integral in equation (20). These are discussed in the following subsection.

## 2.4 Geometrical Factors

### 2.4.1 Apparent surface

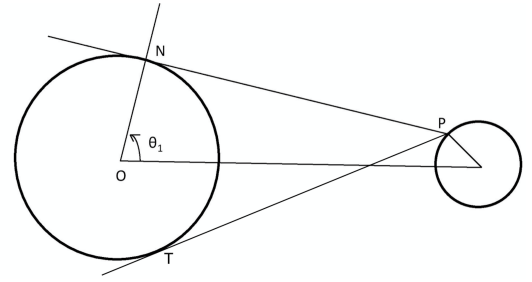


Figure 2. Tangents to the stellar surface PN and PT determine the integral limit or the surface visible to the observer

The apparent surface of the host star visible to a close-in planet depends on the star-planet distance. If the planet is far enough from the star, one can see the entire hemisphere of the star. However, as we approach closer, we only see a region bound between the tangents to the stellar circle from the point of observation on the planet. Fig. 2 demonstrates that a tangent from a point P on the planet determines the limit of what is visible to the observer. The angle  $\theta_1$  hence determines the limit of integration. The procedure to calculate  $\theta_1$  is as follows.

Using the coordinates introduced in the previous subsection, we substitute  $\phi = 0$  since the calculation is limited to the YZ plane. The slope of the tangent NP is given by:

$$m_1 = \frac{z_s - z_p}{y_s - y_p}. \quad (35)$$

Therefore,

$$m_1 = \frac{R \sin \theta - r \sin \lambda}{R \cos \theta - (a + r \cos \lambda)}. \quad (36)$$

Since the tangent and normal to the stellar circle are perpendicular to each other, the slope of the normal to the stellar

circle(ON) can be calculated using the general relation between the slopes of two mutually perpendicular lines with slopes  $m_1$  and  $m_2$ , that is :

$$m_1 m_2 = -1. \quad (37)$$

Therefore, slope of ON is given by,

$$m_2 = \tan \theta = \frac{a + r \cos \lambda - R \cos \theta}{R \sin \theta - r \sin \lambda}. \quad (38)$$

To simplify equation 38, we first divide both numerator and denominator by  $\cos \theta$  :

$$\tan \theta = \frac{(a + r \cos \lambda) \sec \theta - R}{R \tan \theta - r \sin \lambda \sec \theta}. \quad (39)$$

After rearranging terms, we have:

$$R \tan^2 \theta - r \sin \lambda \sec \theta \tan \theta = (a + r \cos \lambda) \sec \theta - R \quad (40)$$

$$R \sec \theta = r \sin \lambda \tan \theta + a + r \cos \lambda. \quad (41)$$

Now we square this expression and define  $\beta = a + r \cos \lambda$ . Consequently, we get:

$$\sec^2 \theta (R^2 - r^2 \sin^2 \lambda) - 2\beta R \sec \theta + \beta^2 + r^2 \sin^2 \lambda = 0. \quad (42)$$

Solving this quadratic equation and assuming  $\beta \sim a$  we get:

$$\cos \theta = \cos \theta_1 = \frac{R \pm r \sin \lambda}{a}. \quad (43)$$

The above solution represents both tangents from the given point P. It should be noted that equation (43) accommodates all possible cases of the star-planet system, including hypothetical cases that are less likely to be found observationally. For all practical purposes, we can ignore the radius of the planet in equation (43) without appreciably changing the results. We can now calculate  $\theta_1$  at any given value of  $\lambda$  and can express the formula for irradiance as:

$$I = \int_{-\theta_1}^{\theta_1} \int_{-\theta_1}^{\theta_1} \frac{L_b \cos \theta d\theta d\phi}{4\pi^2} \frac{\cos A \cos \psi}{d_s^2}. \quad (44)$$

#### 2.4.2 Stellar surface above local horizon

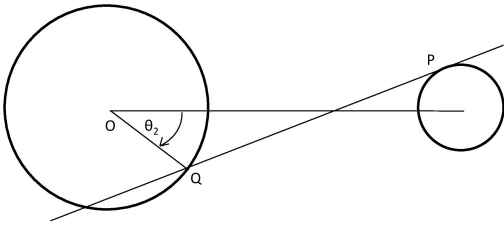


**Figure 3.** The point of intersection of the local horizon PQ with the stellar circle constraints the lower limit of the integral

For higher latitudes on close-in exoplanets, a part of the stellar surface is hidden beneath the local horizon. This is

taken into account by integrating the surface above the local horizon. In Fig. 3, we can see that the stellar surface below Q lies beneath the local horizon PQ and is hence neglected. Since an incident ray grazing through the local horizon would be perpendicular to the normal vector through that point on the planet, therefore, to obtain the corresponding angle( $\theta_2$ ) determined by the point of intersection of the local horizon with the stellar circle, we put  $\cos A = 0$  in equation (27). Again, we neglect  $\phi$  and only consider the polar angle ( $\theta$ ). When we solve specifically for  $\theta$ , we get a quadratic equation with the following roots:

$$\cos \theta_2 = \frac{\cos \lambda ((r + R + d) \cos \lambda - r)}{R} \pm \frac{\sin \lambda (R^2 - (a \cos \lambda - r)^2)^{1/2}}{R}.$$

$\theta_2$  obtained from the above equation determines the limit of integration for higher latitudes. Therefore, equation (44) now becomes:

$$I = \int_{-\theta_2}^{\theta_1} \int_{-\theta_1}^{\theta_1} \frac{L_b \cos \theta d\theta d\phi}{4\pi^2} \frac{\cos A \cos \psi}{d_s^2}. \quad (45)$$

For brevity, we use  $\forall$  symbol to imply for all.

$\forall \pi - \lambda > 0$ ,  $\theta_2$  is given by:

$$\cos \theta_2 = \frac{\cos \lambda ((r + R + d) \cos \lambda - r)}{R} + \frac{\sin \lambda (R^2 - (a \cos \lambda - r)^2)^{1/2}}{R},$$

while  $\forall \pi - \lambda < 0$ . We have:

$$\cos \theta_2 = \frac{\cos \lambda ((r + R + d) \cos \lambda - r)}{R} - \frac{\sin \lambda (R^2 - (a \cos \lambda - r)^2)^{1/2}}{R}.$$

Equation (44) in this case would be

$$I = \int_{-\theta_1}^{\theta_2} \int_{-\theta_1}^{\theta_1} \frac{L_b \cos \theta d\theta d\phi}{4\pi^2} \frac{\cos A \cos \psi}{d_s^2} \quad (46)$$

$\forall \pi - \lambda > \theta_1$ , one of the polar angle limits will be modified to  $\theta_2$ . In addition to this, another intricacy needs to be addressed. After a certain latitude, the lower limit of the integral will be positive since the local horizon will intersect the star above its equatorial plane. The latitude at which the lower limit is zero is given by  $\pi/2 - \theta_3$ , as shown in Fig. 4.

Therefore,  $\forall \pi - \lambda > \pi/2 - \theta_3$ , equation (45) becomes:

$$I = \int_{\theta_2}^{\theta_1} \int_{-\theta_1}^{\theta_1} \frac{L \cos \theta d\theta d\phi}{4\pi^2} \frac{\cos A \cos \psi}{d_s^2}. \quad (47)$$

The angle  $\theta_3$  can be calculated using basic trigonometry as,

$$\sin \theta_3 = \frac{r}{r + d}. \quad (48)$$

However, this factor only comes into play when the planet is so close that the distance between the stellar and planetary surface is comparable to the planetary radius.

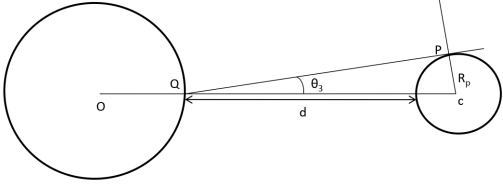


**Figure 4.** Lower limit of the integral becomes positive after a certain latitude on the planet determined by  $\pi/2 - \theta_3$

### 2.4.3 Critical point of symmetry

The critical point of symmetry is the point after which we expect to see differences from the inverse-square law. The equation for the critical point of symmetry can be simply calculated by calculating  $\theta_2$  at a point where it touches the stellar circle instead of intersecting it. In other words, the local horizon will be a common interior tangent to the stellar and planetary circles. The latitude at which the local horizon will be a tangent to the star is given by:

$$\lambda = \cos^{-1} \left[ \frac{R+r}{a} \right] \quad (49)$$

The point along the sub-stellar longitude with the above latitude is termed as the critical point of symmetry. Without loss of generality, we can conclude that all critical points on the planet that make an equivalent angle constitute a critical belt of symmetry.

### 2.5 Limb Darkening

The linear limb darkening law is simply incorporated in the model by rewriting the intensity at a given optical depth as:

$$I(\mu) = I(0)[1 - u(1 - \mu)], \quad (50)$$

with  $\mu = \cos \psi$ . For Sun-like stars, the bolometric limb darkening coefficient is approximately 0.6 (Pannekoek 1935) and the temperature relation with optical depth is given using the Milne-Eddington approximation:

$$T(\tau) = T_{\star} \left[ \frac{3\tau + 2}{4} \right]^{1/4}. \quad (51)$$

Therefore, the general equation culminates to:

$$I = \int_{-\theta_n}^{\theta_n} \int_{-\theta_n}^{\theta_n} \frac{\sigma T_0^4 R^2 \cos \theta \cos A \cos \psi (1 - u(1 - \mu)) d\theta d\phi}{\pi(d_s)^2},$$

where  $T_0$  is the temperature at an optical depth of 1 and  $\theta_n$  depends on the latitude on the planet. A similar equation has been derived by (Wilson 1990) for binary star systems except in his analysis he also includes non-spherical stellar shapes and reflection effects which are ignored in our analysis. The limb darkening has negligible effect on the nature of the irradiance pattern.

### 2.6 General equation for the inverse-square law

In order to compare the results of the model with the inverse-square law, we first calculate the angle of incidence from a point-sized source onto a given point on a planet with latitude  $\lambda$ :

$$\tan i = \frac{a \tan \lambda \cos \lambda}{a \cos \lambda - r}. \quad (52)$$

The distance between them will be given by:

$$d_c = (a^2 + r^2 - 2ar \cos \lambda)^{1/2}. \quad (53)$$

Therefore, we can write the final form of the inverse-square law as:

$$I = \frac{L_b \cos i}{4\pi(a^2 + r^2 - 2ar \cos \lambda)}, \quad (54)$$

where

$$i = \tan^{-1} \left[ \frac{a \tan \lambda \cos \lambda}{a \cos \lambda - r} \right]. \quad (55)$$

The latitude at which  $i$  becomes 90 is termed as the terminator limit for the inverse-square law since the irradiance predicted by the IS law after this point is zero. A consequence of equation (52) is that for a significant size of the planet, the angle at which the irradiance goes to zero is less than 90 degrees.

### 3. Results

We present the results in Fig. 6 for some close Earth-like exoplanets with host stars that have effective temperatures in the range of 5500–6000 K where the linear limb darkening is a good approximation. (Diaz-Cordoves and Giménez 1992)

We find that, at the poles, we get non-zero radiation. The IS law predicts zero irradiance at the poles since it follows a cosine relation of irradiance with latitude. Therefore, for a latitude of 90 degrees, the irradiance becomes zero. Our model takes into account the correct angle made by all surface elements on the star with the point on the planet under consideration, and hence gives accurate, non-zero irradiance values. Fig. 5(a) shows the difference of irradiance values predicted by this model with the values predicted by the IS law at the poles. The difference increases with increasing stellar radius and decreasing semi-major axes. This means that the relative size of the star from the planet plays the key role. The terminator is defined as the locus of points on the exoplanet where the common tangents of both the stellar and planetary spheres touches the planet.

We also find that the day-night terminator is not at the poles but at a latitude greater than 90 degrees. The irradiance becomes zero at around 105–110 degrees latitude for close exoplanets. Mathematically, the terminator angle can be calculated from the slope of the exterior common tangent of the stellar and planetary circles :

$$A_t = \pi/2 + \sin^{-1} \left[ \frac{R-r}{a} \right]. \quad (56)$$

From the above equation, it is evident that the angle is higher for higher host-star radius and lower semi-major axis-and-planetary radius. Fig. 5(b) shows the maximum latitude up to

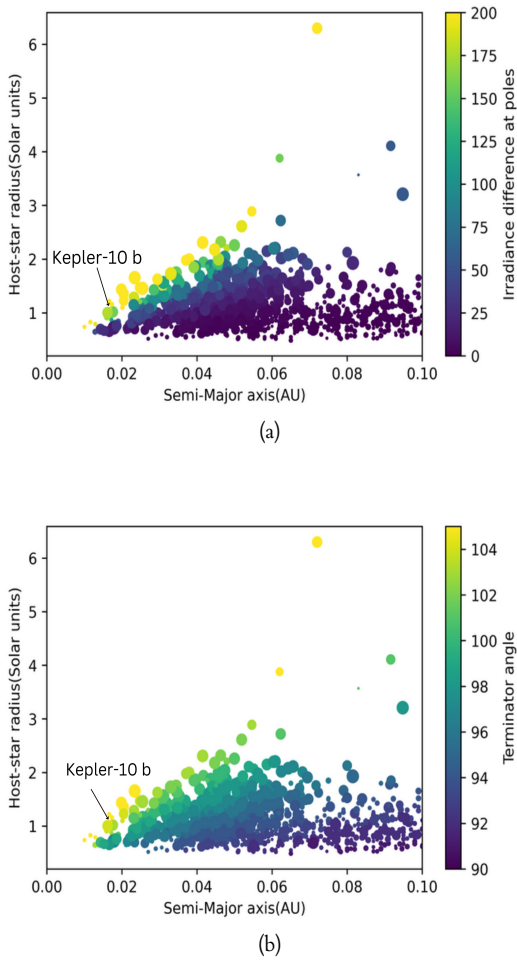


**Figure 5.** Fig (a) depicts the irradiance at the poles for the two approaches in  $\text{kW/m}^2$  for the current population of exoplanets with host-star effective temperatures between 4000 and 7000 K and spot size proportional to the planetary size. Kepler-10 b is hiding exactly behind the green dot in this plot. Fig (b) depicts the angle of the terminator from the equator. (Sadh and Gavassino 2022)

which irradiance is non-zero or the terminator angle value from the equator. For the current population of exoplanets, we find that the angle can extend up to 110 degrees from the equator or 20 degrees from the pole to the night-side. We also present the result for an extreme hypothetical case in Fig. 7. If the Earth were to be at a distance of 0.5 % of its present distance from the Sun, we can expect to see deviations from the inverse-square variation for latitudes as low as 30 degrees. Additionally, the terminator will shift much farther towards the night side of the exoplanet, and virtually the whole planetary surface will receive the stellar radiation leaving only a small portion in the dark. Such a case is only a mathematical possibility and not likely to exist in reality and is merely presented to demonstrate the extremity of the deviations. Since climate is a non-linear dynamical system, small changes in irradiance can lead to completely different climate states and habitability conditions (Forget and Leconte 2014; Kilic, Raible, and Stocker 2017). The extent of difference in irradiation from

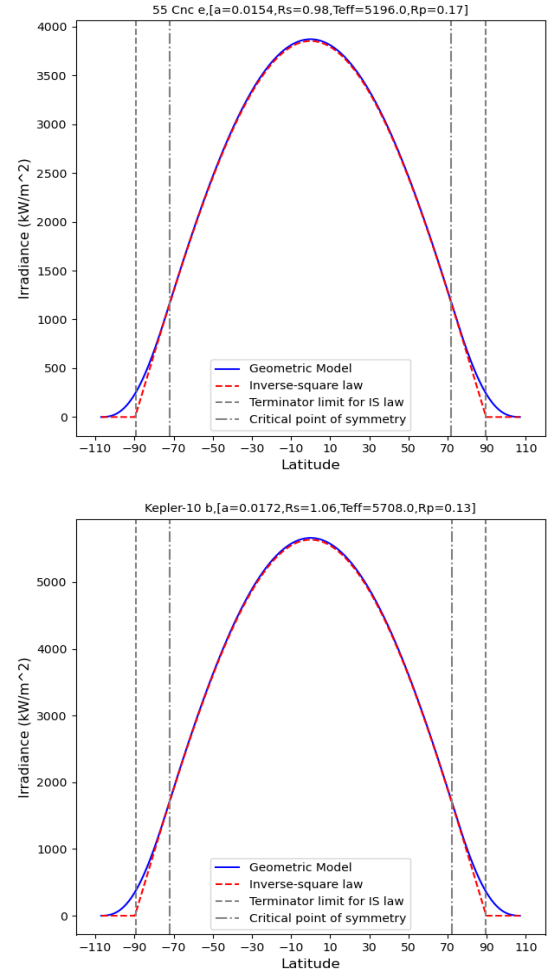


**Figure 6.** Irradiation for close-in, Earth-sized planets, 55 Cnc e and Kepler-10b which are examples of the extreme cases of this effect.

the standard approach at the poles seems significant enough and is therefore likely to introduce appreciable changes in the current climate models of close-in Earth-size exoplanets. Exoplanets at such a close distance are likely to be tidally locked to their host stars. For such systems, it has been earlier proposed that the region near the terminator might be hospitable for life since the temperatures on either hemispheres will be too extreme (Singal 2014). It would be interesting to speculate the existence of life on the night-side of such exoplanets since from the calculations, we see that irradiance close to the poles towards the night-side would be Earth-like and in this belt of hospitable conditions it would be reasonable to expect habitable environment. However, only a climate model incorporating these geometric effects with the atmospheric and oceanic factors could provide a more credible basis for

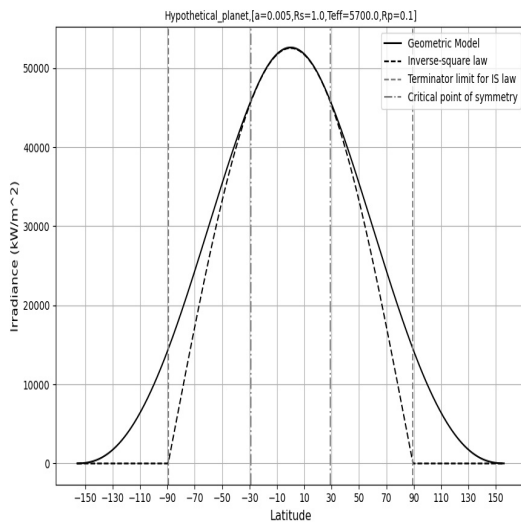


**Figure 7.** A hypothetical planet configuration with a Earth-sized planet at an extremely close distance of 0.005 AU to a Solar-size star.

assessing habitability of such planets. A recent study (Lobo et al. 2023) does an extensive study on terminator habitability. This strengthens our case and applicability of our model. The python code *InstellCa* uses the stellar and planetary parameters from the extra-solar planet encyclopedia (Schneider et al. 2011) and the NASA exoplanet archive (Akeson et al. 2013) to compute the irradiance plots. Currently, the model assumes a linear limb darkening law, and therefore works best for Sun-like stars. The *InstellCa* code is openly available for users<sup>a</sup>.

### Acknowledgement

I would like to thank Prof. Mark Wardle for his feedback and comments on the paper.

Competing Interests None

Data Availability Statement The code for analysing the exoplanet data can be accessed on GitHub.

### References

- Akeson, RL, X Chen, D Ciardi, M Crane, J Good, M Harbut, E Jackson, SR Kane, AC Laity, S Leifer, et al. 2013. The nasa exoplanet archive: data and tools for exoplanet research. *Publications of the Astronomical Society of the Pacific* 125 (930): 989.
- Batalha, Natalie M, William J Borucki, Stephen T Bryson, Lars A Buchhave, Douglas A Caldwell, Jørgen Christensen-Dalsgaard, David Ciardi, Edward W Dunham, Francois Fressin, Thomas N Gautier III, et al. 2011. Kepler's first rocky planet: kepler-10b. *The Astrophysical Journal* 729 (1): 27.
- Charbonneau, David, and Robert W Noyes. 2000. Present and near-future reflected light searches for close-in planets. *Arxiv preprint astro-ph/0002489*.

a. <https://github.com/Mradumay137/InstellCa>

- Demory, B-O, Michaël Gillon, D Deming, D Valencia, S Seager, B Benneke, Christophe Lovis, P Cubillos, J Harrington, KB Stevenson, et al. 2011. Detection of a transit of the super-earth 55 cancri e with warm spitzer. *Astronomy & Astrophysics* 533:A114.
- Diaz-Cordoves, J, and A Giménez. 1992. A new nonlinear approximation to the limb-darkening of hot stars. *Astronomy and Astrophysics* 259:227–231.
- Forget, François, and Jeremy Leconte. 2014. Possible climates on terrestrial exoplanets. *Philosophical Transactions of the Royal Society A: Mathematical, Physical and Engineering Sciences* 372 (2014): 20130084.
- Guillot, Tristan. 2010. On the radiative equilibrium of irradiated planetary atmospheres. *Astronomy & Astrophysics* 520:A27.
- Horvat, Martin, Kyle E Conroy, David Jones, and Andrej Prša. 2019. Bolometric treatment of irradiation effects: general discussion and application to binary stars. *The Astrophysical Journal Supplement Series* 240 (2): 36.
- Huang, He-qing, and Dao-qi Zhou. 2000. The effect of irradiation absorption on an ellipsoidal component of a close binary. *Chinese Astronomy and Astrophysics* 24 (3): 339–348.
- Kane, Stephen R, Tiffany Jansen, Thomas Fauchez, Franck Selsis, and Alma Y Ceja. 2020. Phase modeling of the trappist-1 planetary atmospheres. *arXiv preprint arXiv:2012.00080*.
- Kilic, Cevahir, CC Raible, and TF Stocker. 2017. Multiple climate states of habitable exoplanets: the role of obliquity and irradiance. *The Astrophysical Journal* 844 (2): 147.
- Kingston, Robert H. 1995. *Optical sources, detectors, and systems: fundamentals and applications*. Academic Press.
- Kopal, Zdeněk. 1954. Photometric effects of reflection in close binary systems. *Monthly Notices of the Royal Astronomical Society* 114 (1): 101–117.
- Léger, A, D Rouan, Jodi Schneider, P Barge, M Fridlund, B Samuel, M Ollivier, E Guenther, M Deleuil, HJ Deeg, et al. 2009. Transiting exoplanets from the corot space mission-viii. corot-7b: the first super-earth with measured radius. *Astronomy & Astrophysics* 506 (1): 287–302.
- Lobo, Ana H, Aomawa L Shields, Igor Z Palubski, and Eric Wolf. 2023. Terminator habitability: the case for limited water availability on m-dwarf planets. *The Astrophysical Journal* 945 (2): 161.
- Mayor, Michel, and Didier Queloz. 1995. A jupiter-mass companion to a solar-type star. *Nature* 378 (6555): 355–359.
- Mihalas, Dimitri, and Barbara Weibel Mihalas. 1984. *Foundations of radiation hydrodynamics*.
- Misner, C. W., K. S. Thorne, and J. A. Wheeler. 1973. *Gravitation*.
- Pannekoek, A. 1935. Limb darkening. *Monthly Notices of the Royal Astronomical Society* 95:733.
- Sadh, Mradumay, and Lorenzo Gavassino. 2022. Extended body corrections to the inverse square law for spherically symmetric sources. In *XI polish astronomical society meeting*, edited by Ewa Szuszkiewicz, Agnieszka Majczyna, Katarzyna Małek, Milena Ratajczak, Ewa Niemczura, Urszula Bąk-Stęślicka, Radosław Poleski, Maciej Bilicki, and Łukasz Wyrzykowski, 12:270–273. October.
- Schneider, Jean, Cyrill Dedieu, Pierre Le Sidaner, Renaud Savalle, and Ivan Zolotukhin. 2011. Defining and cataloging exoplanets: the exoplanet.eu database. *Astronomy & Astrophysics* 532:A79.
- Singal, Ashok K. 2014. Life on a tidally-locked planet. *arXiv:1405.1025*.
- Wilson, RE. 1990. Accuracy and efficiency in the binary star reflection effect. *The Astrophysical Journal* 356:613–622.



## Appendix 1. Violation of the inverse-square law

We start from the fundamental question which motivates this paper: when is the inverse-square law violated? To answer this question, we will use a simple geometrical argument based on the conservation of the energy.

### Appendix 1.1 The energy of radiation

Let us, first of all, recall some basics of radiation kinetic theory. The photon gas, with specific intensity  $I_\nu$  (Misner, Thorne, and Wheeler 1973), has an associated stress-energy tensor (Mihalas and Weibel Mihalas 1984)

$$R^{\alpha\beta} = c^{-1} \int_0^{+\infty} dv \oint d\Omega I_\nu(\mathbf{n}) n^\alpha n^\beta, \quad (57)$$

which, in vacuum (in the limit of weak gravitational fields), obeys the conservation law

$$\partial_\alpha R^{\alpha\beta} = 0. \quad (58)$$

If we set  $\beta = 0$  in this equation, we obtain

$$\partial_t \varepsilon + \nabla \cdot \mathbf{F} = 0, \quad (59)$$

where we have introduced the radiation energy density and energy flux vector as respectively

$$\varepsilon = R^{00} \quad F^j = R^{0j}. \quad (60)$$

If we work in the stationary limit, we finally find

$$\nabla \cdot \mathbf{F} = 0. \quad (61)$$

This is the radiation-energy conservation condition, which approximately holds in the space which surrounds stars and planets. If we consider an arbitrary Gaussian 2D surface  $\Sigma$  which does not contain matter, but only radiation, then equation (61) implies

$$\oint_\Sigma \mathbf{F} \cdot d\boldsymbol{\Sigma} = 0. \quad (62)$$

We will use this formula to see where the inverse-square law is valid and where it is not, by appropriately choosing  $\Sigma$ .

### Appendix 1.2 The method of the solid angle

Throughout the paper, we will focus for simplicity on a binary system, comprised of a star and a single planet. Both the objects are approximated as perfectly spherical. In addition, since we are interested only in computing the energy that the star is transferring to the planet, we will treat the latter as a perfect absorber, namely we will not consider the contributions to  $\mathbf{F}$  due to emission and reflection of the planet (which are beyond the scope of the paper and would require us to model the atmosphere of the planet in detail).

To probe the validity of the inverse-square law, we construct a Gaussian 2D surface as follows (see figure 8):

- We consider an infinitesimal solid angle  $\delta\Omega$  which is centered in the center of the star and points towards the planet, intersecting a small portion of its surface we call this intersection  $\Sigma_P$  and we orient it from the star to the planet.

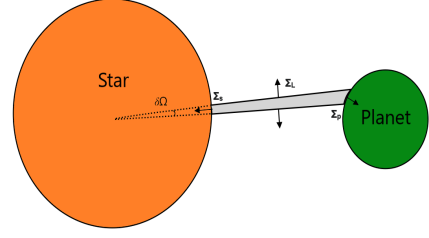


**Figure 8.** Schematic representation of the Gaussian 2D surface constructed in subsection Appendix 1.2. An infinitesimal solid angle  $\delta\Omega$  is centered in the center of the star and reaches the surface of the planet. Along its path, it “cuts out” a portion of space between the star and the planet whose boundary is the surface under consideration. The arrows in the picture are the normal unit vectors to the surface.

- We call  $\Sigma_S$  the portion of the surface of the star that intersects  $\delta\Omega$  and we orient it from the planet to the star.
- We call  $\Sigma_L$  the lateral surface of the solid angle crossing the vacuum between the star and the planet and we orient it outwardly.
- $\Sigma_P \cup \Sigma_L \cup \Sigma_S$  is a connected Gaussian outwardly oriented surface which encloses a volume containing only radiation. This volume is the vacuum region between the star and the planet that intersects the solid angle.

Applying the energy conservation condition (62) to  $\Sigma_P \cup \Sigma_L \cup \Sigma_S$ , we obtain

$$\int_{\Sigma_P} \mathbf{F} \cdot d\boldsymbol{\Sigma} + \int_{\Sigma_L} \mathbf{F} \cdot d\boldsymbol{\Sigma} + \int_{\Sigma_S} \mathbf{F} \cdot d\boldsymbol{\Sigma} = 0. \quad (63)$$

On the other hand, if  $L_b$  and  $R_*$  are respectively the bolometric luminosity and the radius of the star, we have (recalling the orientation conventions we imposed)

$$\int_{\Sigma_S} \mathbf{F} \cdot d\boldsymbol{\Sigma} = -\frac{\delta\Omega}{4\pi} L_b. \quad (64)$$

In addition, since  $\Sigma_P$  is infinitesimal, we can make the approximation

$$\int_{\Sigma_P} \mathbf{F} \cdot d\boldsymbol{\Sigma} \approx \mathbf{F}_P \cdot \boldsymbol{\Sigma}_P, \quad (65)$$

where  $\mathbf{F}_P$  is  $\mathbf{F}$  evaluated in the center of  $\Sigma_P$  and  $\boldsymbol{\Sigma}_P$  is the normal area vector associated with  $\Sigma_P$ . Therefore, equation (63) can be equivalently rewritten in the form

$$\mathbf{F}_P \cdot \boldsymbol{\Sigma}_P = \frac{\delta\Omega}{4\pi} L_b - \int_{\Sigma_L} \mathbf{F} \cdot d\boldsymbol{\Sigma}. \quad (66)$$

We are going to show that, depending on the position of  $\Sigma_P$ , equation (66) might reduce to inverse-square law or might be in contradiction with it.

### Appendix 1.3 A sufficient condition for the inverse-square law to hold

To find those regions, on the surface of the planet, where (66) reduces to the inverse-square law, we consider the following argument.



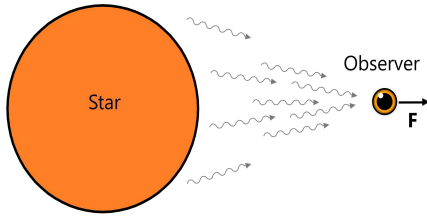


**Figure 9.** If there is no obstacle between the star and the observer, the energy flux  $\mathbf{F}$  points along the axis that connects them. In fact, by symmetry, for every photon that is not collinear to this axis, on average there is another one with opposite transverse momentum, as shown in the picture.

Take a point (in the vacuum space) from which the star is entirely visible, i.e. none of its surface is eclipsed by the planet. By symmetry, it is clear that, on this point, the energy flux emitted by the star points radially (referring to a coordinate system which is centered in the center of the star), see figure 9. From this we can conclude that, if the star is entirely visible from all the points of the Gaussian surface  $\Sigma_P \cup \Sigma_L \cup \Sigma_S$ , then

$$\mathbf{F}_P = F_P \hat{\mathbf{r}} \quad \text{and} \quad \int_{\Sigma_L} \mathbf{F} \cdot d\boldsymbol{\Sigma} = 0, \quad (67)$$

where  $\hat{\mathbf{r}}$  is the unit radial vector. The second equation is motivated by the fact that  $\hat{\mathbf{r}} \cdot d\boldsymbol{\Sigma} = 0$  on  $\Sigma_L$ , see figure 8. If we insert (67) into (66) and use the condition

$$\hat{\mathbf{r}} \cdot \boldsymbol{\Sigma}_P = d_c^2 \delta\Omega, \quad (68)$$

which holds by construction ( $d_c$  is the distance of  $\Sigma_P$  from the center of the star), we obtain the inverse-square law for the energy current:

$$F_P = \frac{L_b}{4\pi d_c^2}. \quad (69)$$

Finally, if we call  $\hat{\mathbf{v}}$  the unit normal vector to  $\Sigma_P$  and use it to define the geometric quantity

$$\cos i := \hat{\mathbf{r}} \cdot \hat{\mathbf{v}}, \quad (70)$$

then, using (65) and (69), we obtain the inverse-square law for the intensity:

$$I := \lim_{\delta\Omega \rightarrow 0} \left[ \frac{1}{\delta\Omega} \int_{\Sigma_P} \mathbf{F} \cdot d\boldsymbol{\Sigma} \right] = \frac{L_b \cos i}{4\pi d_c^2}. \quad (71)$$

In conclusion, we have found that a sufficient condition for the inverse-square law to hold is that the star is completely visible (i.e. not eclipsed) from all the points of the Gaussian surface  $\Sigma_P \cup \Sigma_L \cup \Sigma_S$ . We are finally able to understand where the inverse-square law ceases to hold.

Consider an arbitrary point  $x$  in any of the white regions of figure 10. It is evident that no obstacle stands between a hypothetical observer sitting on  $x$  and the star, which is thus completely visible from  $x$ . On the other hand, if we choose  $\delta\Omega$  in such a way that  $\Sigma_P$  is located on the light-green

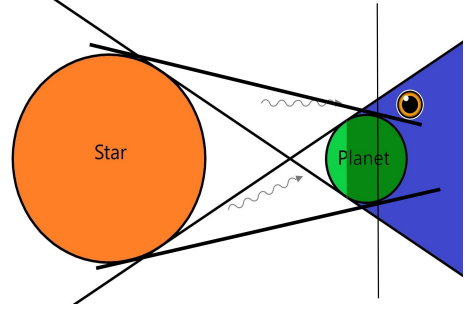


**Figure 10.** The blue region is the set of all those positions from which the star is not entirely visible. An observer (represented in our case by the eye) sitting on an arbitrary blue point would see a partially eclipsed star. Since in this case some of the photons directed to the observer are screened by the planet, the flux  $\mathbf{F}$  fails to be radial. This opens the door to possible violations of the inverse-square law on the dark green region of the planet. However, one should note that the violations are only expected where the flux from the star is non-zero. For instance in the region on the planet beyond the common tangents, the flux is naturally zero.

section of the planet's surface, the associated Gaussian surface  $\Sigma_P \cup \Sigma_L \cup \Sigma_S$  lays in the white region entirely, we can therefore, conclude that the inverse-square law must be valid on the light-green spherical dome of the planet.

In contrast, consider an observer in the blue region of figure 10, e.g. the eye we included in the image. This observer is not able to see the whole star. As a consequence, the flux fails to be radial. On the other hand, if we choose  $\delta\Omega$  in such a way that  $\Sigma_P$  is located on the dark-green section of the planet's surface (see figure (10)), a fraction of the Gaussian surface  $\Sigma_P \cup \Sigma_L \cup \Sigma_S$  (including  $\Sigma_P$  itself) necessarily lays in the blue region of space we can, therefore, conclude that there is room for violations of the inverse-square law only on the dark-green spherical dome of the planet, as equations (67) no longer apply.

The position at which the light-green region of the planet (where the inverse-square law is valid) meets the dark-green region (where the inverse-square law ceases to hold) will be called in this paper *critical belt of symmetry* and each point of it is a *critical point of symmetry* we choose this name because these points mark the transition line at which the symmetry argument that justifies the inverse square starts being invalid. An analytical formula for the position of the critical belt of symmetry will be given later. From the perspective of an observer walking on the surface of the planet, the critical points of symmetry are all those positions from which the circular boundary of the star seems to touch the horizon.